



This is a repository copy of *Agent-based simulator of dynamic flood-people interactions*.

White Rose Research Online URL for this paper:
<https://eprints.whiterose.ac.uk/150005/>

Version: Published Version

Article:

Shirvani, M., Kesserwani, G. and Richmond, P. (2021) Agent-based simulator of dynamic flood-people interactions. *Journal of Flood Risk Management*, 14 (2). e12695. ISSN 1753-318X

<https://doi.org/10.1111/jfr3.12695>

Reuse

This article is distributed under the terms of the Creative Commons Attribution (CC BY) licence. This licence allows you to distribute, remix, tweak, and build upon the work, even commercially, as long as you credit the authors for the original work. More information and the full terms of the licence here:
<https://creativecommons.org/licenses/>

Takedown

If you consider content in White Rose Research Online to be in breach of UK law, please notify us by emailing eprints@whiterose.ac.uk including the URL of the record and the reason for the withdrawal request.



eprints@whiterose.ac.uk
<https://eprints.whiterose.ac.uk/>

Agent-based simulator of dynamic flood-people interactions

Mohammad Shirvani¹ | Georges Kesserwani¹  | Paul Richmond²

¹Department of Civil and Structural Engineering, University of Sheffield, Mappin St, Sheffield City Centre, Sheffield, UK

²Department of Computer Science, University of Sheffield, Mappin St, Sheffield City Centre, Sheffield, UK

Correspondence

Georges Kesserwani, Department of Civil and Structural Engineering, University of Sheffield.

Email: g.kesserwani@sheffield.ac.uk

Funding information

Engineering and Physical Sciences Research Council, Grant/Award Number: EP/R007349/1

Abstract

This article presents a simulator for the modelling of the two-way interactions between flooding and people. The simulator links a hydrodynamic model to a pedestrian model in a single agent-based modelling platform, Flexible Large-scale Agent Modelling Environment for the Graphical Processing Unit (FLAMEGPU). Dynamic coupling is achieved by the simultaneous update and exchange of information across multiple agent types. Behavioural rules and states for the pedestrian agents are proposed to account for the pedestrians' presence/actions in/to floodwater. These are based on a commonly used hazard rate (HR) metric to evaluate the risk states of people in floodwater, and by considering two roles for the pedestrians: *evacuees* or *responders* for action *during* or *before* the flood event, respectively. The potential of the simulator is demonstrated in a case study of a flooded and busy shopping centre for two scenarios: (a) during a flood evacuation and (b) pre-flood intervention to deploy a sandbag barrier. The evacuation scenario points to changes in floodwater hydrodynamics around congested areas, which either worsen (by 5–8%) or lessen (by 25%) the HR. The intervention scenario demonstrates the utility of the simulator to select an optimal barrier height and number of responders for safe and effective deployment. Accompanying details for software accessibility are provided.

KEYWORDS

coupled agent-based models, evaluation of flood evacuation and mitigation strategies, flood risk analysis, human response dynamics

1 | INTRODUCTION

Flooding is a frequent hazard that can disrupt communities, in particular in small urban areas (<0.5 km × 0.5 km) where people congregate. These areas usually include important pedestrian hubs such as in or around shopping centres, supermarkets, transport infrastructure, and football stadiums (Becker et al., 2015). Although computational models have become central to mitigate, prepare and manage flood risks (Kreibich, Seifert, Merz, &

Thieken, 2010; Kreibich, Bubeck, van Vliet, & de Moel, 2015; Wedawatta & Ingirige, 2012), there is a particular strategic need to develop a simulation framework and models for integrating human behaviour dynamics into the flood risk analysis (Aerts et al., 2018; Lumbroso & Vinet, 2012; McClymont, Morrison, Beevers, & Carmen, 2019; Zischg, 2018).

Agent-based models (ABMs) offer a flexible method to develop a computational model to simulate the co-evolution of the actions and interactions of multiple

This is an open access article under the terms of the Creative Commons Attribution License, which permits use, distribution and reproduction in any medium, provided the original work is properly cited.

© 2021 The Authors. *Journal of Flood Risk Management* published by Chartered Institution of Water and Environmental Management and John Wiley & Sons Ltd.

drivers that could lead to the emergent behaviour of receptors (Bonabeau, 2002). This provides the ability to dynamically explore the synergies between social and physical dynamics and mitigation policies, making ABMs ideally suited to support flood resilience studies at different scales (spatial, temporal, and organisational). In recent years, ABMs have been devised to support flood risk management, most commonly at meso and macro scales (Lumbroso, Gaume, Logtmeijer, Mens, & van der Vat, 2008), to simulate and analyse various receptors' response to floodwater. For example, ABMs have been developed to evaluate: risk management strategies under future climate change scenarios with multiple institutional drivers (Abebe, Ghorbani, Nikolic, Vojinovic, & Sanchez, 2019; Jenkins, Surminski, Hall, & Crick, 2017); business loss and long-term effect of floods on economic growth (Grames, Prskawetz, Grass, Viglione, & Blöschl, 2016; Li & Coates, 2016); and, the effect of protection measures, individual behaviour and flood frequency on the resilience of at-risk communities (Tonn & Guikema, 2018). ABMs have also been built for flood evacuation planning in coastal areas, to estimate evacuation times for dam failures, and to estimate the number of casualties and injuries (Aboelata & Bowles, 2008; Dawson, Peppe, & Wang, 2011; Liu & Lim, 2016; Lumbroso & Davison, 2018; Lumbroso, Sakamoto, Johnstone, Tagg, & Lence, 2011; Mas et al., 2015).

For flood risk analysis in small and congregated urban areas, only a few ABMs have been designed for the evaluation of evacuation strategies considering the emergent behaviour of individual people in response to a flood. Liu, Okada, Shen, and Li (2009) devised an ABM to simulate the movement of up to five evacuees in an underground station during a flash flood, while interacting with each other and responding to the station's layout and the flood information available. Bernardini et al. (2017) designed "FloodPEDS": an ABM incorporating a crowd of pedestrians responding to evolving floodwater under evacuation scenarios. In FloodPEDS, pedestrian movement in floodwater has been modelled via (sparse) data processed from video footage of people stuck in floodwater. The modelled data was incorporated into a standard pedestrian simulation model. Such models combine a local motion planning model (i.e., *social force model*) with a global path planning model (i.e., a *navigation map*). The *social force model* accounts for the movements of each individual and by modelling the interaction between individuals to derive forces that avoid collisions with neighbours. Whereas, the *navigation map* encodes the features of the walkable area necessary for the individuals' *way-finding decisions* (Jiang, Chen, Li, & Ding, 2020; Li, Wei, & Xu, 2019), for example, terrain obstacles and walls that need to be

avoided as the individuals navigate and vector fields providing navigation to key destinations. More generally, the life safety model (LSM, www.lifesafetymodel.net) has been developed to assess the risk of flooding on people while taking into account dynamic interactions between multiple receptors across different scales. The LSM incorporates interactions between vehicles, via a traffic model, and includes a pedestrian flow model accounting for people movement as they relay warnings to each other (Lumbroso & di Mauro, 2008; Lumbroso et al., 2011; Lumbroso, Simm, Davison, White, & Durden, 2015; Lumbroso & Davison, 2018). Similarly, the LifeSIM model (www.hec.usace.army.mil/software/hec-lifesim) was developed to include an individuals' response to emergency warnings and their interaction with each other and their surroundings, for example, urban layouts and buildings, to estimate fatalities under flood-induced evacuation conditions. However, these ABMs are applied to support modelling problems at relatively large spatial scales, where the presence of people will not have a significant impact on floodwater depths and velocities (>5 km × 5 km). Also, they are not dynamically coupled to a hydrodynamic model. This may be needed to incorporate local changes in the floodwater hydrodynamics in response to the people movement in confined areas of mass gatherings, for example, groupings during an emergency evacuation, or changes in the height of the ground elevation in response to targeted people actions, for example, as they act as sandbaggers. For small and congregated urban areas, such people responses can actually affect the floodwaters, and thus developing a fully coupled "flood-pedestrian" simulator in a single ABM platform is necessary to be able to capture two-way interactions between people and flooding.

This article presents the development and evaluation of a "flood-pedestrian" simulator, which dynamically couples a hydrodynamic model to a pedestrian model on the Flexible Large-scale Agent Modelling Environment for the Graphical Processing Unit (FLAMEGPU) (Section 2.1). The FLAMEGPU platform allows discrete and continuous agent types to be defined, and to dynamically give-and-take copies of the data stored across multiple ABMs (Section 2.2). The hydrodynamic model is incorporated on a grid of fixed agents (Section 2.3), referred to as flood agents, which is coincident with the *navigation map* of the pedestrian evacuation model (Section 2.4). The latter involves continuous pedestrian agents driven by a *social force model* and moving on the *navigation map* spanned by a fixed grid of navigation agents. Dynamic passing of information across the pedestrian and flood agents is facilitated by the navigation agents (Section 2.5). Behaviour rules governing pedestrian interaction with/to the flood hydrodynamics are

implemented based on one of the two different roles that pedestrians can be assigned: *evacuees* moving in floodwater where the presence of individuals and groups of people are incorporated by changing the surface roughness coefficient in the hydrodynamic model; or, *responders* participating in pre-event sandbagging where the sandbags are incorporated by changing the height of the ground elevation parameter in the hydrodynamic model. The dynamic coupling ability of the proposed simulator is demonstrated over a synthetic case study of a flooded and crowded shopping centre considering two scenarios: (a) during a flood evacuation (Section 3.1), and (b) pre-flood intervention to deploy a temporary flood barrier (Section 3.2). Simulation results are discussed considering the broader implications on flood evacuation and intervention strategies for small and congregated urban studies. Conclusions are drawn reflecting on the future research needs (Section 4), and the details for accessing the simulator software are provided in the acknowledgments section.

2 | MATERIALS AND METHODS

2.1 | Overview of FLAMEGPU

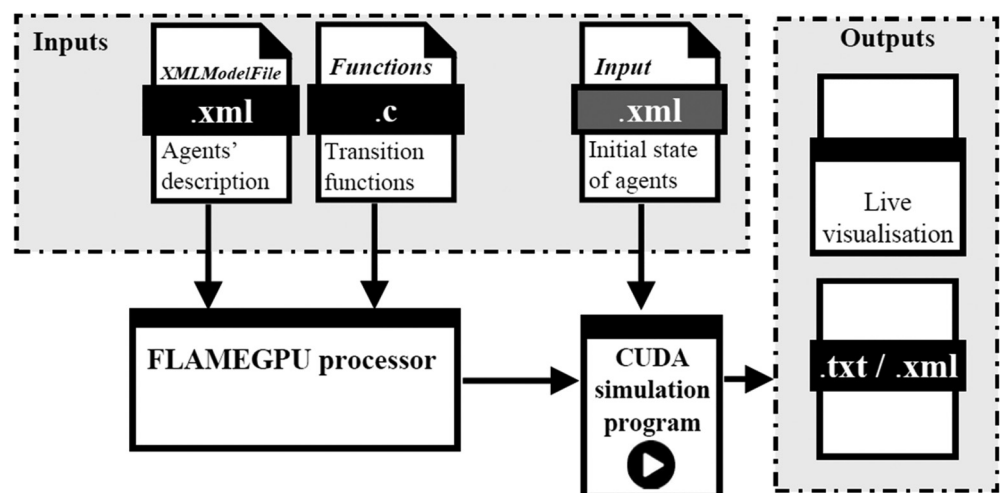
FLAMEGPU is a computational platform for the simulation of multiple agent interactions on CUDA Cores for parallel processing on graphical processing units (GPUs) (Chimeh & Richmond, 2018; Richmond, Coakley, & Romano, 2009). It involves a standard procedure to create and run a CUDA simulation program by processing three inputs, as shown in Figure 1. The *XMLModelFile.xml* is where a user defines formal agent specifications, including their descriptive information, type, numbers, properties, etc. An agent can be specified in space as either *discrete* or *continuous* (FLAMEGPU user guide). *Discrete*

agents have fixed coordinates and must be pre-allocated in the memory of the GPU as two-dimensional (2D) grid of size of a power of two numbers (e.g., 64×64 , 128×128 , 256×256 , 512×512 , etc.). *Continuous agents* change their coordinates and their population; they can be of any population size (within the limitations of available GPU memory). The *input.xml* file contains the initial conditions of the variables of state of all the defined agents. In a *single C script*, the behaviour rules to update all agents are implemented, and include *Transition functions* to achieve dynamic passing of the information stored in the agents as they get simultaneously updated (FLAMEGPU user guide). The implementation of the coupled flood-pedestrian simulator on FLAMEGPU is described next, with a focus on the agent specifications and rules for interactions used across both the hydrodynamic model and the pedestrian model.

2.2 | Agents specifications

The pedestrian model involves two agent types: *navigation agents* and *pedestrian agents*. Navigation agents are defined to be discrete, that is, agents are located on a grid encoding a *navigation map* detailing obstacles and navigation fields for a given study area. Each singular navigation agent stores information that a pedestrian requires to carry on with their movement at the discrete location which it represents. This information in particular, conveys the direction to key destinations and their location on the map (e.g., the entrances, exits, and walkable pathways), and obstacles that pedestrians must avoid (e.g., walls and terrain blocks). For this study, a grid resolution of 128×128 navigation agents is defined to provide pedestrian agents with the information on the location and direction of the entrances/exits and the terrain features in the study area. In this work, this

FIGURE 1 The process for generating and running an agent-based simulation program on flexible large-scale agent modelling environment for the graphical processing unit (FLAMEGPU) (<http://www.flamegpu.com/home>). A detailed list of the agents' description and initial states is available in the accompanying "run guide" document of the flood-pedestrian simulator software (see also the Acknowledgements section)



resolution was found sufficient to capture details of the built environment.

Pedestrian agents are modelled as continuous space agents as they can change position (represented as a continuous value) in space and over time. The space between pedestrian agents is controlled by each one's perceptive steering forces (Karmakharm, Richmond, & Romano, 2010), which ensures that the pedestrian has a physical radius given its continuous location position. In the meantime, the pedestrian agents receive information from the navigation agents that influence their way-finding decisions from the navigation map. Multiple pedestrian agents can be presented at the same time over one mutual navigation agent as they are of continuous type.

A hydrodynamic model, which describes flood agents, is incorporated within FLAMEGPU pedestrian model to enable the dynamic exchange of information between navigation and flood agents. Flood agents are represented using discrete agents, which are coincident with the grid of navigation agents. Each flood agent stores its position x (m) and y (m), terrain properties in terms of height z (m) and Manning's roughness parameter n_M ($\text{s m}^{-1/3}$), and the states of the floodwater variables in terms of water depth h (m) and velocity components u (m/s) and v (m/s). The states of floodwater variables in the flood agent are affected by those stored in the adjacent neighbours sharing its four interfaces. Therefore, each flood agent is programmed to store and exchange information with these four neighbours, in order to simultaneously update the states of the floodwater variables in all the flood agents (Section 2.3).

The information stored in the pedestrian agents and in the flood agents is passed between them through the navigation agents that act as shared communication interfaces (Section 2.5). This means that each navigation agent is set to receive the information of a pedestrian or flood agent at their location and send back an update to the flood agent. That is, a navigation agent converts the information received from the flood agent into a flood hazard rate (HR) quantity, which is retrieved by any pedestrian agent walking in its spatial area. Estimating a flood HR usually involves measuring a product quantity of a water depth h to a velocity magnitude V (Costabile, Costanzo, de Lorenzo, & Macchione, 2020). As in Kvočka, Falconer, and Bray (2016) and Willis, Wright, and Sleigh (2019), the degree of flood HR is estimated as $\text{HR} = (V + 0.5) \times h$, with $V = \max(|u|, |v|)$, following the risk to people method developed for the UK Environment Agency (2006). Pedestrian agents therefore consider a *flood risk state* and a *walking speed state* based on the information of the flood HR they receive at their local and temporal location. Pedestrian agents are also assigned a *role* (Section 2.5) and accordingly pass certain

information to the navigation agent where they are located at a certain time. This is to incorporate any local change in the terrain properties caused by pedestrians' presence or actions, namely: due to local and temporal grouping of *evacuees* in certain zones leading to increasingly higher surface roughness; or, due to sandbagging by *responders* leading to a local change in the height of the terrain. The navigation agent processes the information on such changes, received by the pedestrian agents, and passes them back to the hydrodynamic model to dynamically updates the surface roughness's Manning's parameter (n_M) or the ground elevation (z) in the hydrodynamic model. Then, it passes the updated terrain parameters back to the flood agent at its equivalent position. Section 2.5 follows up with the rules governing the interactions between the flood, navigation, and pedestrian agents.

2.3 | Update of the floodwater states stored in the flood agents

As flood agents in the FLAMEGPU model are distributed on a grid, their states of floodwater variables can be updated by adopting a hydrodynamic numerical model on a mesh formed by square elements (e.g., TUFLOW-HPC, Wang, Liang, Kesserwani, & Hall, 2011). The hydrodynamic model is re-implemented so as to suit the *non-sequential* computation on FLAMEGPU such that it dynamically updates the states of floodwater variables at all the flood agents at the same time (i.e., in parallel).

A hydrodynamic model is selected based on an explicit shock-capturing scheme (Wang et al., 2011), in a first-order formulation to keep the calculation stencil limited to the information stored in the immediate neighbours sharing its four interface (Figure 2). The scheme numerically solves the 2D depth-averaged shallow water equations, including the ground elevation and the Manning's roughness parameter, written in the following vectorial form (Néelz & Pender, 2009):

$$\partial_t \mathbf{U} + \partial_x \mathbf{F} + \partial_y \mathbf{G} = \mathbf{S} \quad (1)$$

In Equation (1), t is the time, $\mathbf{U} = [h, hu, hv]^T$ is the flow vector containing the water depth and components of the unit-width flow discharge, $\mathbf{F} = [hu, hu^2 + \frac{1}{2}gh^2, huv]^T$ and $\mathbf{G} = [hv, huv, hv^2 + \frac{1}{2}gh^2]^T$ are the components of the flux vectors with g being the gravity constant, and $\mathbf{S} = [0, gh(S_{0x} - S_{fx}), gh(S_{0y} - S_{fy})]^T$ is the source vector containing the terrain slopes from the ground elevation ($S_{0x} = -\partial_x z$ and $S_{0y} = -\partial_y z$) and friction terms (S_{fx} and S_{fy}) expressed by the Manning's formula including n_M .

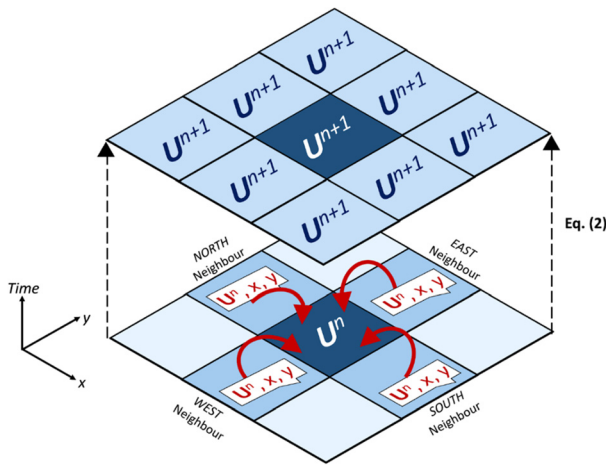


FIGURE 2 A flood agent (“dark blue”) updating its states of floodwater variables, \mathbf{U} , from time iteration n to $n + 1$. The process is done simultaneously for all flood agents, facilitated by the messages (“white message icons”) the flood agent receives to access the states of floodwater variables of its neighbours sharing its four interfaces

For a flood agent at position (x,y) , their vector \mathbf{U} contains constant floodwater states at time iteration n , which need elevating to iteration $n + 1$ according to the following formula (Figure 2).

$$\begin{aligned} \mathbf{U}^{n+1} &= \mathbf{U}^n - \frac{\Delta t}{\Delta x} (\mathbf{F}_{EAST} - \mathbf{F}_{WEST}) - \frac{\Delta t}{\Delta y} (\mathbf{G}_{NORTH} - \mathbf{G}_{SOUTH}) + \mathbf{S} \end{aligned} \quad (2)$$

In Equation (2), Δt , Δx and Δy denote the time step and dimensions of the flood agent. To update the states of floodwater variables in the flow vector \mathbf{U}^n , the incoming and outgoing spatial fluxes across the four interfaces, denoted by \mathbf{F}_{EAST} , \mathbf{F}_{WEST} , \mathbf{G}_{NORTH} , \mathbf{G}_{SOUTH} , and the source vector \mathbf{S} need to be first evaluated. These evaluation are performed while incorporating measures to ensure robust treatments for wetting-and-drying and terrain-slope terms (Wang et al., 2011). As each flood agent (“dark blue,” Figure 2) receives the information (“white message icons,” Figure 2) stored the four neighbours sharing its four interfaces, the robustness treatments alongside flux and source term evaluations can be applied element-wise, that is, to simultaneously update the states of floodwater variables in all the flood agents.

The non-sequential hydrodynamic ABM implementation on FLAMEGPU was verified in reproducing two 2D dam-break flow tests (Huang, Zhang, & Pei, 2013; Wang et al., 2011). In both tests, the hydrodynamic ABM on FLAMEGPU reproduced the same predictions as the

sequential counterpart and shows close agreement alternative predictions (see Appendix for more details).

2.4 | Update of the pedestrian and navigation agents

A pedestrian simulation model has already been implemented in FLAMEGPU (Karmakharm et al., 2010), which has been utilised by this study. It combines a *social force model*, governing random walk movement of the pedestrian agents and their interaction, alongside the navigation agents of the *navigation map* that contains information for the pedestrian agents to find their way in the walkable zones within the study area (Jiang et al., 2020; Li et al., 2019). When there is no floodwater, the walking speed of the pedestrian agents is set to 1.4 m/s to represent the average human walking speed (Mohler, Thompson, Creem-Regehr, Pick, & Warren, 2007; Wirtz & Ries, 1992). Nonetheless, the existing behavioural rules in both the *social force model* and the *navigation map* allow the pedestrian agents to locally increase or decrease their walking speed (e.g., when they need to abruptly change direction to avoid collisions with each other or with existing obstacles located in the study area). The pedestrian simulation model has been adapted into a flood-pedestrian simulator so as to enable exchange of information between the pedestrian and flood agents. It is also adapted to inform on pedestrians-related HR states, changes in local floodwater dynamics as a result of the interactions between the flood, navigation, and pedestrian agents as explained in Section 2.5.

2.5 | Interactions between the flood, navigation, and pedestrian agents

This section explains the behavioural rules programmed to process the information dynamically exchanged between the flood, navigation, and pedestrian agents. Two different sets of pedestrian behavioural rules are implemented depending on the *role* assigned to the pedestrian agents, that is, either to be *evacuees* or *responders*. *Evacuee agents* are pedestrian agents evacuating *during a flood* without a prior warning. Once a non-zero water depth is received by any navigation agent on the navigation map (i.e., from the flood agent at its same location), the pedestrian agents will no longer be entering the study area, and those remaining, that is, the evacuee agents, will be leaving to an emergency exit destination (specified by the user on the navigation map). Evacuee agents in flooded zones receive the flood HR quantity from the navigation agents where they are located.

HR ranges			
From	To	Flood risk state	Walking speed state
0	0.75	Low—safe to walk	1.8 m/s—brisk walk
0.75	1.5	Medium—mildly disrupted	0.9 m/s—slow walk
1.5	2.5	High—disrupted	0.45 m/s—slower walk
2.5	20	Highest—trapped	0.00 m/s—no walk

Abbreviation: HR, hazard rate.

A *flood risk state* is then assigned to each of these evacuee agents based on the four HR ranges used by the UK Environment Agency (2006) for identifying the level of flood risk to people. These ranges define the *low*, *medium*, *high* or *highest* flood risk state of HR (see Table 1). Evacuee agents are also assigned a *walking speed state* that is assumed¹ to be constant per *flood risk state*, such that:

- When an evacuee agent is in a low flood risk state, it is able to accelerate its escape via a brisk walk that is on average 1.8 m/s (Mohler et al., 2007).
- When an evacuee agent is in a medium to high HR flood risk state, it needs to decelerate walking speed to 0.9 and 0.45 m/s, respectively. These walking speeds are within the average range of human walking speeds in floodwater (Lee, Hong, & Lee, 2019).
- When an evacuee agent is at the highest flood risk state, it cannot walk in floodwater due to instability issues and thus has a walking speed of 0 m/s.

Meanwhile, the evacuee agents that are present on the flooded navigation agents are counted: their number, N_p , is used to locally update the Manning's roughness coefficient n_M in the hydrodynamic model as $n_M = n_M + N_p n_M$ (see Figure 3, left). The updated coefficient n_M is then passed back to the flood agent at the navigation agent's location to represent the effects of the presence of individuals and groups of people on floodwater hydrodynamics. For this study, the initial n_M parameter is set to be equal to $0.01 \text{ s m}^{-1/3}$, representative of clear cement (Chow, 1959), and no more than 20 evacuee agents are allowed to simultaneously occupy the area of a navigation agent, which means that any local amendment in n_M cannot exceed $0.2 \text{ s m}^{-1/3}$.

Responder agents form a group of the existing pedestrian agents, who are emergency first responders, taking a series of actions to construct a flood barrier within a specified *time window* due to an advanced flood warning. A standard sandbagging procedure is implemented to form the temporary barrier, which is an appropriate choice to support this study.² To govern the movement and actions of responder agents, destinations of the

TABLE 1 Evacuee agent states in floodwater selected based on the ranges for HR tabulated in the flood hazard matrix of the UK Environment Agency (2006)

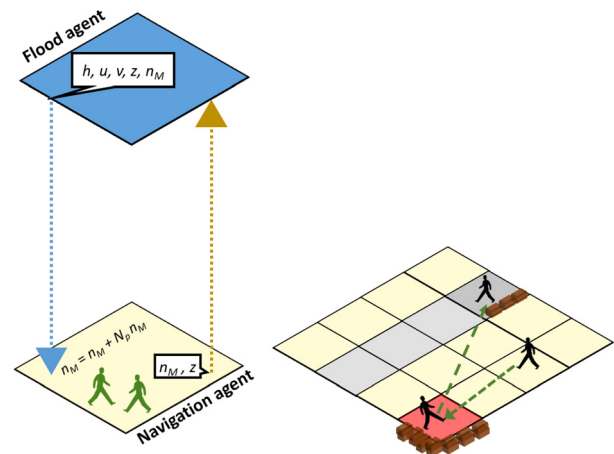


FIGURE 3 Dynamic passing of stored information between a flood agent and pedestrian agents (evacuees) facilitated via the navigation agent that is aligned to the flood agent (left). Procedure for pedestrian agents (responders) deploying a sandbag barrier (right): red navigation agent represents a “sandbag storage” destination and grey navigation agents represent the deployment destination

sandbag storage and of the location of flood barrier are initially specified on the navigation map (Figure 3, right). Responder agents get information to walk to the location of the sandbag storage. Once they reach it, they are set to wait for half a minute representative of a picking up duration (specified), and then pick up the information on the dimension of a sandbag from the navigation agents spanning the sandbag storage location (Figure 3, right). Responder agents are then redirected to carry up this information to the navigation agents spanning the temporary flood barrier, which are set to receive it after a wait of half a minute representative of a safe drop out duration (specified). Responder agents are set to go and share their information with one (specified) first navigation agent representative of the starting location for the deployment. As the dimension of a sandbag is smaller than the area of a navigation agent, the first navigation agent is set to accumulate the received information until it has enough to cover one horizontal layer of sandbags all-over its area. Then, the first navigation agent

increments the ground elevation parameter, z , by one unit of sandbag thickness. The process then moves to the adjacent navigation agent spanning the flood barrier's location, and so on until the single layer of sandbags reach either a wall or an obstacle existing in the study area. Responder agents then repeat the overall process N_L times, until all the navigation agents spanning the flood barrier's location are filled up with N_L (specified) layers of sandbags. After N_L rounds, the height of the ground elevation parameter at the navigation agents spanning the flood barrier's location has become $z \times N_L$. This new height for the ground evaluation is then passed to the flood agents at their aligned location (Figure 3, left), that is, to incorporate the changes from the presence of sandbags in the hydrodynamic model.

3 | DEMONSTRATION ON A SYNTHETIC CASE STUDY

A case study was developed to evaluate the flood-pedestrian simulator for modelling dynamic interactions between people and floodwater flows. The case study utilised a shopping centre filled with people exposed to flooding. It distinguished two independent scenarios one with the *pedestrians* as *evacuees*, and another involving them as *responders*. Scenario 1 assumed that there is no early warning nor an early evacuation plan, and focused on the behaviour of pedestrians as evacuees during the

propagation of the floodwater while moving to an emergency exit (Figure 4a). Scenario 2 focused on mitigation options on the number of the responders and thickness of the flood barrier needed for a safe and effective deployment upstream of the emergency exit (Figure 4b). Scenario 2 also requires a specified lead time, taken to be 12 hr. This time was selected assuming severe flood warnings were issued for the areas surrounding the shopping centre, though the shopping centre had remained open (e.g., as with the case of Meadowhall shopping centre during November 2019 floods, which opened despite an early warning of half-a-day [www.bbc.co.uk/news/uk-50341846]).

The area of the shopping centre is $332 \text{ m} \times 332 \text{ m} = 110,224 \text{ m}^2$ (Figure 4), chosen based on the average area size of the UK's 43 largest shopping centres (Gibson, Percy, Yates, & Sykes, 2018; Globaldata Consulting, 2018; Sen Nag, 2018; Tugba, 2018). The shopping centre includes stores, located at the east and west side, separated by corridors linking the entrance doors to an open area. Through these corridors, pedestrians can enter the open area and walk toward their destinations. The open area was assumed to be occupied by a population of 1,000 pedestrians (configurable by the user) when there is no floodwater. This average population was assumed in spite of an influx of people entering or leaving from seven entrance doors with an equal probability of one in seven. The total walkable area of the shopping centre, including the open area and the corridors, is equal

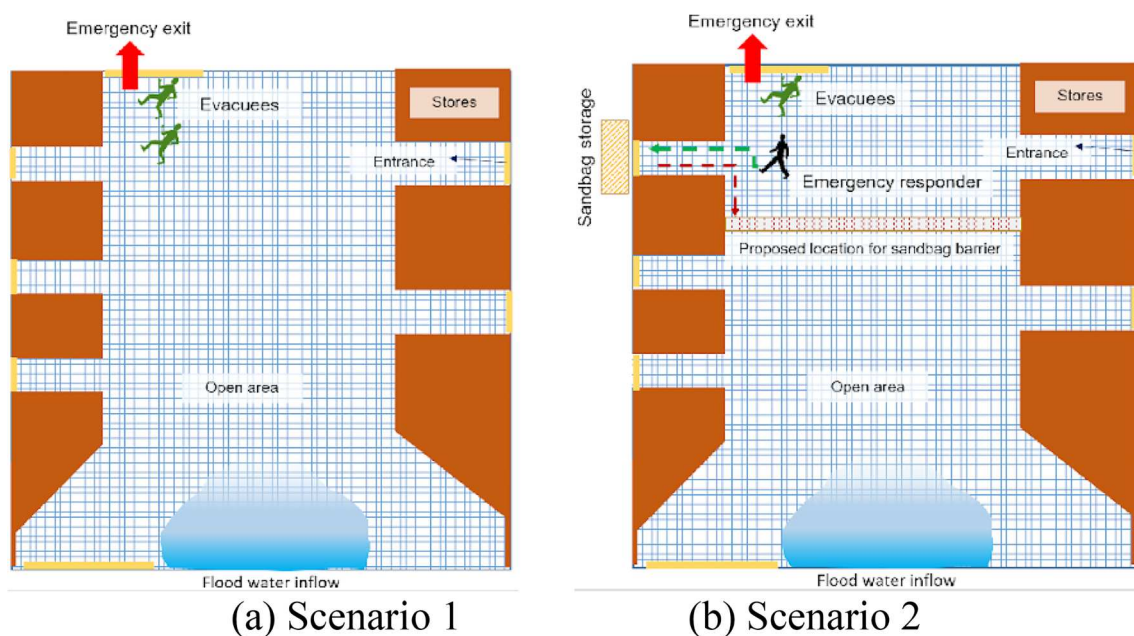


FIGURE 4 Schematic description of the hypothetical shopping centre (Section 3) with the two scenarios: (a) during a flood evacuation; and (b) pre-flood intervention. (a) Scenario 1 and (b) Scenario 2

to 70,350.8 m². A population of 1,000 pedestrians was selected to give an area of almost 8.4 × 8.4 m² for each person. This area allows some areas of the pedestrian space to not be crowded, based on a calculator toolbox of the average space required for individuals in malls (Engineering ToolBox, 2003). The flood propagation was assumed to breach from the southern side along a 100 m width (Figure 4), assuming floodwaters had reached the shopping centre after a severe inundation from a river nearby. When flooding started in Scenario 1, in response to an announcement, pedestrians had started the evacuation to the emergency exit located at the northern side (Figure 4a), which was set to remain open during evacuation.

In Scenario 2, a group of the pedestrians were responders, tasked to deploy a local barrier at the location specified in Figure 4b and within a time window that did not exceed the specified lead time of 12 hr. The area where the intended barrier was 168.6 m long and it has the same width as a navigation agent (i.e., 2.59 m for a grid of 128 × 128 navigation agents). The responders were set to build the barrier by placing layers of sandbags in this area. The dimension of a sandbag was based on standard measurements (Padgham, Horne, Singh, & Moore, 2014; Williamson, 2010), to be 40 cm long × 30 cm wide × 25 cm thick. This means that 3,484 sandbags were needed to form a one-layer thick barrier, which is a close estimate to the sandbag numbers predicted by online calculation tools (e.g., 3,318 sandbags, <https://sandbaggy.com/blogs/articles/sandbag-calculator>), and recommended in the UK official guidance (Environment Agency, 2009).

In both scenarios, the flood-pedestrian simulator model within FLAMEGPU was executed with a resolution of 2.59 m × 2.59 m for the grids of navigation and flood agents. When floodwaters occupy the study area, the time-step is calculated dynamically from the hydrodynamic model under the CFL condition (CFL number = 0.5), while otherwise the 1.0 s time-step of the pedestrian model is selected by default.

3.1 | Flood condition selection based on HR analysis

An *equivalent triangular hydrograph* was used to represent the flooding inflow. This is a standard method reported in hydrology manuals (e.g., United States Department of Agriculture, 2018) and computational hydrology textbooks (e.g., Adrien, 2003). The inflow hydrograph was characterised by a flow peak, Q_{peak} , and a duration, t_{inflow} . Four choices of a flooding inflow hydrograph were explored based on fixing the volume of

water that entered the shopping centre. The Norwich inundation case study reported a population of 500 to 2000 individuals that were flooded in a residential area located 50 m away from a river inundation (Section 6.3.3, document FD2321/TR1, Environment Agency, 2006). Because of its resemblance to the case of the shopping centre, it was considered to calibrate the inflow hydrographs, Q_{peak} for 60 min of flooding, that is, estimated according to initial water depth and velocity magnitude of $h_{inflow} = 1$ m and $v_{inflow} = 0.2$ m/s, respectively. This corresponds to an initial inflow hydrograph with $(Q_{peak}, t_{inflow}) = (20 \text{ m}^3/\text{s}, 60 \text{ min})$ for which $Q_{peak} = v_{inflow} h_{inflow} B$ where $B = 100$ m is the length of the inflow breach. The three other inflow hydrographs were formed to represent more severe flooding events, by recursive halving of t_{inflow} alongside doubling of v_{inflow} ($h_{inflow} = 1$ m is fixed), leading to inflow hydrographs with: $(Q_{peak}, t_{inflow}) = (40 \text{ m}^3/\text{s}, 30 \text{ min})$, $(80 \text{ m}^3/\text{s}, 15 \text{ min})$ and $(160 \text{ m}^3/\text{s}, 7.5 \text{ min})$, respectively, which are shown in Figure 5.

To analyse flood event severity resulting from the four selected inflow hydrographs, the hydrodynamic model within FLAMEGPU was executed with each of the hydrographs. For all simulation runs, the model was applied with slip boundary conditions for the northern side and wall boundary conditions for the eastern and western sides. Figure 6 shows the time history of the maximum HR calculated from the model outputs during 60 min. The inflow hydrographs with $(20 \text{ m}^3/\text{s}, 60 \text{ min})$, $(40 \text{ m}^3/\text{s}, 30 \text{ min})$, and $(80 \text{ m}^3/\text{s}, 15 \text{ min})$, show a maximum HR below 2 and only exceeding 1 between 4 and 6 min. This indicates that these inflow hydrographs lead to flooding that at worst disrupt a few pedestrians for a very short duration of 2 min. In contrast, the inflow hydrograph with $(160 \text{ m}^3/\text{s}, 7.5 \text{ min})$ demonstrates the most severe flooding event with significantly higher maximum HR values³ occurring over a 10 min, that is, indicative of potentially disruptive propagation of floodwaters in the shopping centre. Hence, only the inflow hydrograph with $(160 \text{ m}^3/\text{s}, 7.5 \text{ min})$ was considered when exploring the flood-pedestrian simulator within FLAMEGPU for the proposed Scenarios 1 and 2.

3.2 | Simulation of Scenario 1 (during a flood evacuation)

The flood-pedestrian simulator was applied to simulate Scenario 1. The pedestrian model was set to have a constant rate of 10 entering/leaving pedestrians per entrance/exit such that to maintain a total of 1,000 randomly walking pedestrians before flooding happens. A pre-flooding duration of $t = -5$ min was set in the

FIGURE 5 Flooding inflow hydrographs defined according to four different flow peaks, by fixing the volume of water that can be released into the shopping centre and, doubling the discharge peak (Q_{peak}) while halving the duration of its occurrence (t_{inflow})

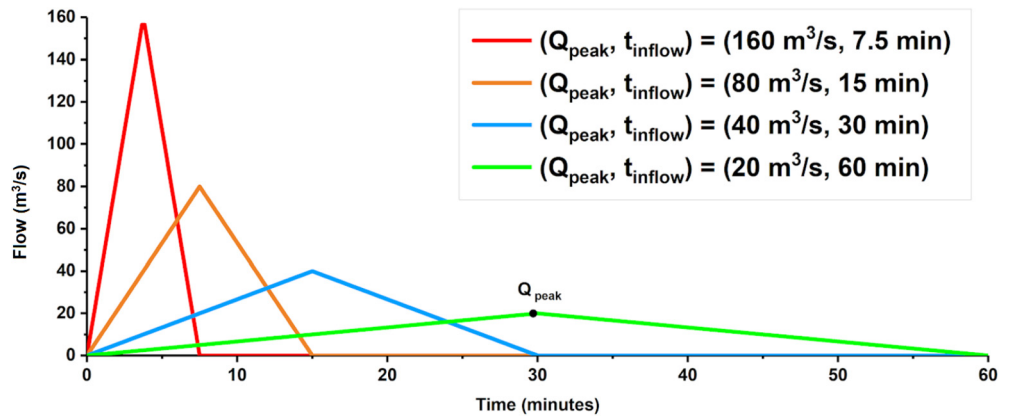
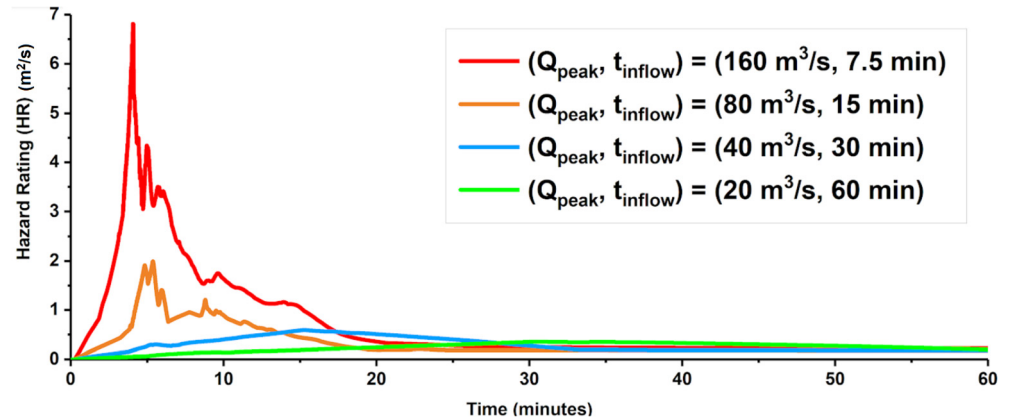


FIGURE 6 Time history of the maximum HR calculated from the model outputs of the hydrodynamic model on flexible large-scale agent modelling environment for the graphical processing unit (FLAMEGPU) run for the four selected inflow hydrographs



hydrodynamic model, by zeroing Q_{peak} , in order to allow spreading of the pedestrians all over the walkable area (blue zone in Figure 4a). When flooding entered the walkable area, at $t = 0$ min, the pedestrian agents were scheduled to become evacuees. The simulation was set to terminate when all evacuees left the walkable area via the emergency exit (Figure 4a). In a single run, the flood-pedestrian simulator was set to record, every 0.1 min, the information stored in the flood agents (coordinate, water depth, water velocity and HR) and the pedestrian agents (coordinate and the HR-related flood risk states). Two runs were performed one “with” and one “without” the effects of people on local floodwater hydrodynamics (Section 2.5). The time history of the outputs produced by the two runs is compared in Figure 7, in terms of statistics of the flood risk states (Table 1) of evacuees.

Before 2.8 min, both runs led to almost similar statistics indicating that 60% of the evacuees were either in a dry zone or in a state of low HR, while the remaining 40% were at most in a medium HR state. After 2.8 min and before 4.9 min, at least 55% of the evacuees had medium to highest HR states, namely in the vicinity of 3.6 min where 5–8% more pedestrians were identified to be in high to highest HR states for the run “with” the effects of people on local floodwater hydrodynamics

(compare Figure 7a to Figure 7b). For the latter run, more pedestrians with the highest HR states were noted, and this was likely caused by the relative local increase in the HR due to the grouping of pedestrians at critical zones and times (see also Figure 8 and its discussions). After 4.9 min and before 8.0 min, the majority of the evacuees had a medium HR state, namely in the vicinity of 6.3 min. Over this duration, 25% more pedestrians were found to be in a state of low HR, for the same run “with” the effects of people on local floodwater hydrodynamics (compare Figure 7a to Figure 7b), due to a relatively local decrease in the HR. After 8.0 min, all the evacuees had a low HR state, irrespective of the run and were able to continue the evacuation process until it ended after 10 min. Notably, as the evacuees become congested on their way to the emergency exit, they affect their surrounding evacuees to become: either in a *higher* risk state of HR when the evacuees were in a *state of high to highest HR*, or in a *lower* risk state of HR when the evacuees were in a *state of medium HR*.

This aspect can be closely explored in the spatial plots of Figure 8 for the runs “without” and “with” the effects of people on local flood hydrodynamics, respectively, after 3.6 and 6.3 min (Figure 8a,b). The plots include the 2D spatial flood maps in terms of HR and the evacuees.

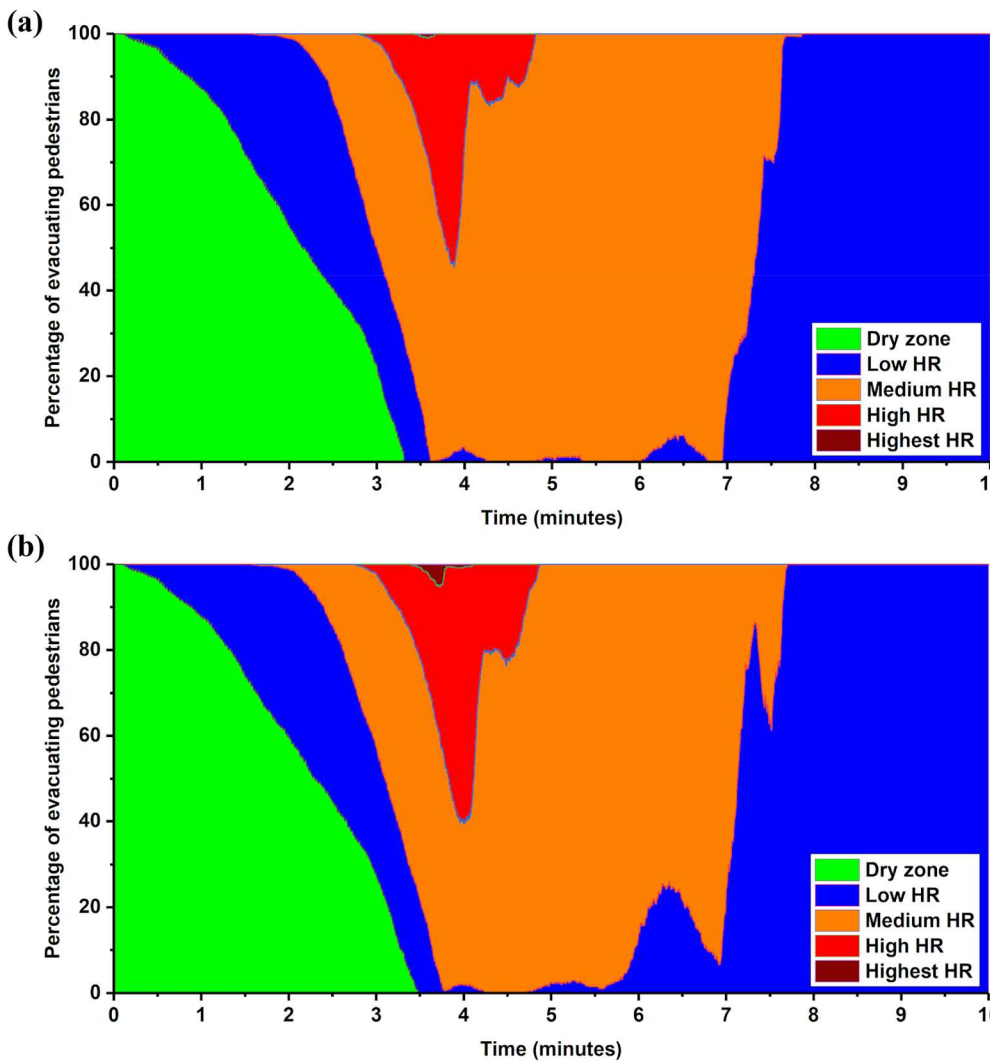


FIGURE 7 A stack chart illustrating the “flood risk states” (Table 1) of the pedestrians as they evacuate during 10-min flooding, without (a), and with (b) accounting for the effects of people on local floodwater hydrodynamics

Comparing the left and right columns in Figure 8a, a clear difference can be observed between the distribution of the evacuees and the flood maps in the crowded zones of the shopping centre: around the middle, more evacuees had high to highest HR states and the local flood hydrodynamics was relatively higher. Whereas, closer to the emergency exit downstream, more evacuees had a low HR state indicative of relatively lower local flood hydrodynamics. The latter observation can also be detected when comparing the left and right columns in Figure 8b. Overall, these results indicate that the local synergies between flood and evacuees can dramatically affect flood impact on evacuee states in floodwater.

3.3 | Simulation of Scenario 2 (pre-flood intervention)

The flood-pedestrian simulator was applied to simulate Scenario 2, with the aim to identify a minimum required

number of people and thickness for the barrier for a safe and effective deployment within a safety time window of 12 hr. Four group sizes for the responders were explored, made of 50, 100, 200, and 300 pedestrians, respectively, alongside six layers of thickness for the sandbag barrier. Hence, a total of 24 simulations were run to estimate the deployment time for a barrier up to six-layer thick and considering the four group sizes. Per group size, a first simulation started with the responders evacuating as soon as they had completed a one-layer thick barrier for flood risk analysis to be applied; then, by analogy, a second simulation was run to analyse the case for a two-layer thick barrier, and so on until the case of a six-layer thick barrier was analysed. The analysis also considered the respective changes in floodwater hydrodynamics in relation to the water depth and maximum HR as the barrier’s thickness is increased. In Figure 9, the simulated time taken to deploy up to a six-layer thick (sandbag) barrier are shown for the four group sizes for the emergency responders. As shown in Figure 9, within the safety time

FIGURE 8 Spatial flood maps alongside the distribution of evacuees at (a) $t = 3.6$ min and (b) $t = 6.3$ min: Left and right columns contain the plots produced by the run “without” and “with” the effects of people on local flood hydrodynamics, respectively

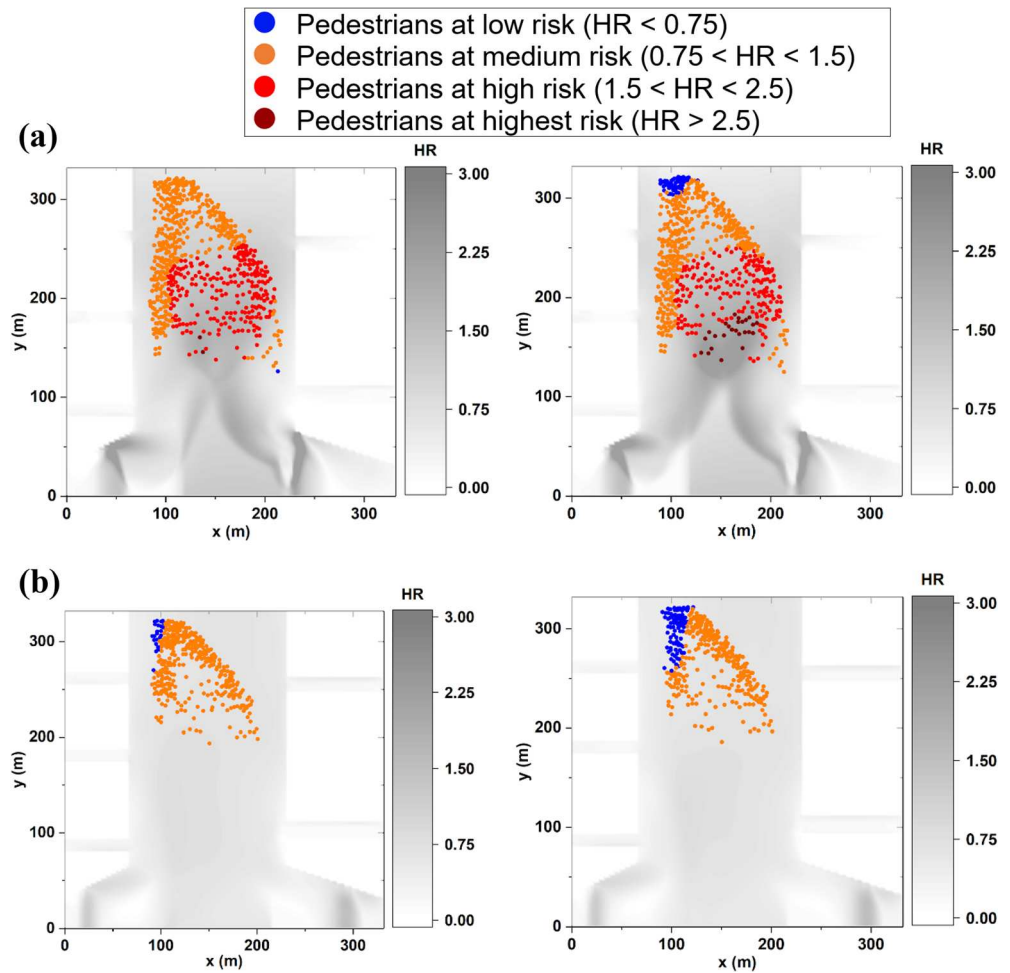
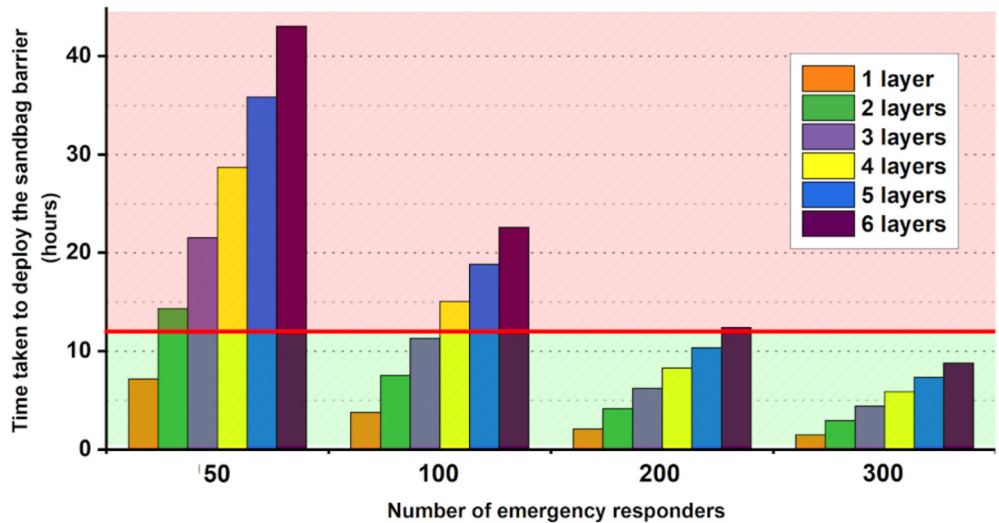


FIGURE 9 Simulated times versus responders' group size for deploying up to six-layer thick (sandbag) barrier: “red line” indicates flooding start time below which is safe to deploy (area shaded in “green”) or otherwise unsafe (area shaded in “red”)



window (“green” area of less than 12 hr): the group of 50 responders could only deploy a one-layer thick barrier, the groups of 100 and 200 responders could deploy a barrier between three- to five-layer thick, respectively; whereas, the group of 300 responders could deploy up to six-layer thick barrier. It is worth noting that involving

higher group sizes may not be realistic and was found to result in efficiency stagnation due to overcrowding.⁴

Figure 10 shows the changes in water depth as the barrier's thickness is increased: water depth downstream of the barrier reduced to around 0.4 m with one-layer thickness, to around 0.3 m with two-layer thickness and

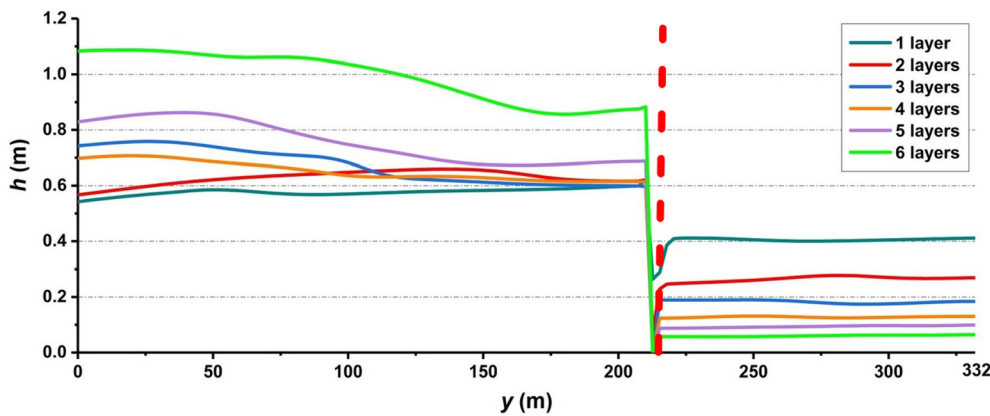


FIGURE 10 Centrelines of two-dimensional (2D) water depth maps along y -axis after the deployment the sandbag barrier (red dashed line) considering up to six layers of sandbag thickness

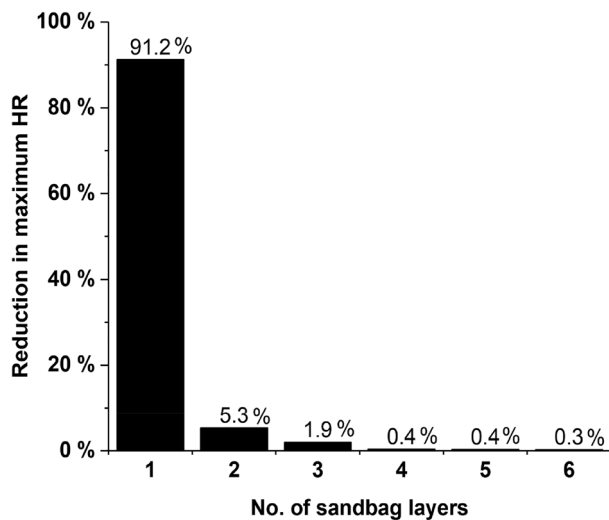


FIGURE 11 Cumulative percentage of maximum HR reduction in line with increased thickness of the barrier in terms of number of sandbag layers

to less than 0.2 m with tree-layer thickness and higher. To help assess the level of safety attributed to these water depths, it is further necessary to analyse their respective velocity impacts as recommended by the Environment Agency (2006, p. 13).

Figure 11 illustrates the relative change in maximum HR downstream of the barrier with respect to the barrier's thickness level in terms of number of sandbag layers. After a one-layer thick barrier, a major drop of 91.2% in maximum HR is observed, which is quite expected relative to having no barrier at all. After two- and three-layer thickness, more relative reduction of 5.3 and 1.9%, respectively, is observed for the maximum HR. After four-layer thickness, no further significant reduction in maximum HR is noted ($\sim 0.4\%$), suggesting that there is no point in going beyond three layers to reduce the flood risk to potentially walking pedestrians downstream of the barrier.

Overall, the combined analyses of Figures 9–11 seem to suggest that a three-layer thick barrier (0.75 m height) would be sufficient to alleviate the flood impacts upstream of the emergency exit of the shopping centre, and its deployment is feasible within less than 12 hr by involving a group of responders made up of 100 people.

4 | CONCLUSIONS AND OUTLOOK

The FLAMEGPU platform was used to dynamically couple validated hydrodynamic and pedestrian models, forming a “flood-pedestrian” simulator. The pedestrian model involved continuous pedestrian agents moving based on the information available on the *navigation map* formed by a grid of navigation agents while following a standard *social force model*. A grid of flood agents was coincident with the grid of navigation agents, on which the states of floodwater variables are stored and updated by a hydrodynamic model. Dynamic passing of information across the pedestrian and flood agents was facilitated by the navigation agents. Behaviour rules governing pedestrian interaction with/to the flood hydrodynamics were implemented for two roles that pedestrians can be assigned: *evacuees* moving in floodwater where the presence of individuals and groups of people was incorporated by changing the surface roughness coefficient in the hydrodynamic model; and, *responders* that participate in pre-event sandbagging where the sandbags were incorporated by changing the height of the ground elevation parameter in the hydrodynamic model. The functioning of the flood-pedestrian simulator was demonstrated over a synthetic case study of a flooded and densely populated shopping centre for two scenarios: (a) during a flood evacuation to an emergency exit, and (b) pre-flood intervention to deploy, from sandbags, a temporary flood barrier. The simulation results of Scenario 1 identified that incorporating local effects of

evacuees on floodwater hydrodynamics can dramatically affect flood impact on the flood risk states of evacuee in relatively confined areas. This dramatic change in flooding impact was noted to be extreme: either reduced the risk to the surrounding of a group of people when the people were in low to medium state of flood HR, or increased the risk when people were located in the highest state of flood HR. The simulation results of Scenario 2 provided evidence that the flood-pedestrian simulator can also be used to decide on the required number of people for emergency first responders and the required minimum height for a temporary flood barrier for a safe and effective deployment, alongside a quantification of the resulting level of flood risk reduction. These simulation results suggest a potential utility of the flood-pedestrian simulator to inform emergency evacuation and intervention strategies for relative small-scale and congregated areas such as supermarkets, football stadiums or shopping centres.

Work is ongoing to support the simulator with more realistic in-model human behaviour rules to floodwater, that is, variable body shapes and height for the pedestrians, variable people walking speeds and stability rules (Shirvani et al., 2020), and to demonstrate its potential to plan mass emergency evacuation for a real study site. There is also a crucial need for interdisciplinary research across social science and psychology, hydraulic engineering and modelling, computer science, and system engineering to characterise and formulate hydro-social behavioural rules that would feature in such a flood-people simulator.

ACKNOWLEDGEMENTS AND SOFTWARE ACCESSIBILITY

The authors declare that there is no conflict of interest. This work was supported by the UK Engineering and Physical Sciences Research Council (EPSRC) grant EP/R007349/1. The authors thank Mozghan Kabiri Chimeh and Peter Heywood from the Research Software Engineering (<https://rse.shef.ac.uk/>) group for providing technical support during the implementation of the flood-pedestrian simulator on FLAMEGPU. The authors also thank the two anonymous reviewers for their careful reading and their insightful comments and suggestions that greatly improved the quality of this article. The flood-pedestrian simulator software is available on DAFNI (<https://dafni.ac.uk/project/flood-people-simulator/>), where it can be run from a graphical interface and supported by a detailed “run guide” document. Further updates on ongoing developments related to the flood-pedestrian simulator can be found on www.seamlesswave.com/Flood_Human_ABM.

ENDNOTES

- ¹ This assumption is sufficient to support to scope of this investigation. Variable walking speed and stability rules are feasible options (e.g., Bernardini, Quagliarini, D’Orazio, & Brocchini, 2020; Chen, Xia, Falconer, & Guo, 2019). Exploring their impact on pedestrian evacuation dynamics in floodwater and recovery times is the subject of another study (Shirvani, Kesserwani, & Richmond, 2020).
- ² To demonstrate the feasibility of the coupled ABMs. More efficient sandbag replacement systems (Lankenau, Massolle, Koppe, & Krull, 2020) can also be implemented, tested and compared in a future study.
- ³ Because the aim of this study aimed to explore people effects on local flood hydrodynamics, considering inflow hydrographs that would lead to $HR > 7$ (i.e., indicative of loss of life) was out of scope.
- ⁴ No significant reduction in deployment times was observed as people-group sizes is increase further. This is likely because longer waiting times were needed with higher number of responders.

DATA AVAILABILITY STATEMENT

Data sharing is not applicable to this article as no new data were created or analysed in this study.

ORCID

Georges Kesserwani  <https://orcid.org/0000-0003-1125-8384>

REFERENCES

- Abebe, Y. A., Ghorbani, A., Nikolic, I., Vojinovic, Z., & Sanchez, A. (2019). A coupled flood-agent-institution modelling (CLAIM) framework for urban flood risk anagement. *Environmental Modelling & Software*, *111*, 483–492.
- Aboelata, M., & Bowles, D. S. (2008). LIFESim: A tool for estimating and reducing life-loss resulting from dam and levee failures. In *Proceedings of the Association of State Dam Safety Officials “Dam Safety 2008” Conference*, pp. 533–547. 7–11 September 2008, Indian Wells, CA.
- Adrien, N. G. (2003). *Computational hydraulics and hydrology: An illustrated dictionary*. Boca Raton, FL: CRC Press.
- Aerts, J. C., Botzen, W. J., Clarke, K. C., Cutter, S. L., Hall, J. W., Merz, B., ... Kunreuther, H. (2018). Integrating human behaviour dynamics into flood disaster risk assessment. *Nature Climate Change*, *8*(3), 193.
- Becker, J. S., Taylor, H. L., Doody, B. J., Wright, K. C., Grunfest, E., & Webber, D. (2015). A review of people’s behavior in and around floodwater. *Weather, Climate, and Society*, *7*(4), 321–332.
- Bernardini, G., Postacchini, M., Quagliarini, E., Brocchini, M., Cianca, C., & D’Orazio, M. (2017). A preliminary combined simulation tool for the risk assessment of pedestrians’ flood-induced evacuation. *Environmental Modelling & Software*, *96*, 14–29.
- Bernardini, G., Quagliarini, E., D’Orazio, M., & Brocchini, M. (2020). Towards the simulation of flood evacuation in urban

- scenarios: Experiments to estimate human motion speed in floodwaters. *Safety Science*, 123, 104563.
- Bonabeau, E. (2002). Agent-based modelling: Methods and techniques for simulating human systems. *Proceedings of the National Academy of Sciences*, 99(Suppl 3), 7280–7287.
- Chen, Q., Xia, J., Falconer, R. A., & Guo, P. (2019). Further improvement in a criterion for human stability in floodwaters. *Journal of Flood Risk Management*, 12(3), e12486.
- Chimeh, M. K., & Richmond, P. (2018). Simulating heterogeneous behaviours in complex systems on GPUs. *Simulation Modelling Practice and Theory*, 83, 3–17.
- Chow, V. T. (1959). *Open channel hydraulics*. New York, NY: McGraw-Hill.
- Costabile, P., Costanzo, C., de Lorenzo, G., & Macchione, F. (2020). Is local flood hazard assessment in urban areas significantly influenced by the physical complexity of the hydrodynamic inundation model? *Journal of Hydrology*, 580, 124231.
- Dawson, R. J., Peppe, R., & Wang, M. (2011). An agent-based model for risk-based flood incident management. *Natural Hazards*, 59(1), 167–189.
- Engineering ToolBox. (2003). Room Area per Person. [online]. Retrieved from https://www.engineeringtoolbox.com/number-persons-buildings-d_118.html.
- Environment Agency. (2009). Sandbags and how to use them properly for flood protection. Document FLHO0309BPSL-E-E.
- Environment Agency/DEFRA. (2006). *R&D outputs: Flood risks to people: Phase 2 FD2321/TR1. The flood risks to people methodology*. Bristol: The Flood and Coastal Defence R&D Programme.
- Gibson, A., Percy, J., Yates, D., & Sykes, T. (2018). UK Shopping Centres the Development Story January 2018 [online]. Cushmanwakefield. Retrieved from <http://www.cushmanwakefield.co.uk/en-gb/research-and-insight/2018/uk-shopping-centres-the-development-story-january-2018>.
- Globaldata Consulting. (2018). Top 50 UK Shopping Centres Report [online]. GlobalData. Retrieved from <https://www.globaldata.com/ground-breaking-report-sheds-new-light-uks-best-performing-shopping-centres>.
- Grames, J., Prskawetz, A., Grass, D., Viglione, A., & Blöschl, G. (2016). Modelling the interaction between flooding events and economic growth. *Ecological Economics*, 129, 193–209.
- Huang, Y., Zhang, N., & Pei, Y. (2013). Well-balanced finite volume scheme for shallow water flooding and drying over arbitrary topography. *Engineering Applications of Computational Fluid Mechanics*, 7(1), 40–54.
- Jenkins, K., Surminski, S., Hall, J., & Crick, F. (2017). Assessing surface water flood risk and management strategies under future climate change: Insights from an agent-based model. *Science of the Total Environment*, 595, 159–168.
- Jiang, Y., Chen, B., Li, X., & Ding, Z. (2020). Dynamic navigation field in the social force model for pedestrian evacuation. *Applied Mathematical Modelling*, 80, 815–826.
- Karmakharm, T., Richmond, P., & Romano, D. M. (2010). Agent-based large scale simulation of pedestrians with adaptive realistic navigation vector fields. *TPCG*, 10, 67–74.
- Kreibich, H., Bubeck, P., van Vliet, M., & de Moel, H. (2015). A review of damage-reducing measures to manage fluvial flood risks in a changing climate. *Mitigation and Adaptation Strategies for Global Change*, 20(6), 967–989.
- Kreibich, H., Seifert, I., Merz, B., & Thieken, A. H. (2010). Development of FLEMOcs—A new model for the estimation of flood losses in the commercial sector. *Hydrological Sciences Journal—Journal des Sciences Hydrologiques*, 55(8), 1302–1314.
- Kvočka, D., Falconer, R. A., & Bray, M. (2016). Flood hazard assessment for extreme flood events. *Natural Hazards*, 84(3), 1569–1599.
- Lankenau, L., Massolle, C., Koppe, B., & Krull, V. (2020). Sandbag replacement systems—A nonsensical and costly alternative to sandbagging? *Natural Hazards & Earth System Sciences*, 20(1), 197–220.
- Lee, H. K., Hong, W. H., & Lee, Y. H. (2019). Experimental study on the influence of water depth on the evacuation speed of elderly people in flood conditions. *International Journal of Disaster Risk Reduction*, 39, 101198.
- Li, C., & Coates, G. (2016). Design and development of an agent-based model for business operations faced with flood disruption. *Complex Systems: Fundamentals & Applications*, 90, 275.
- Li, M., Wei, Y., & Xu, Y. (2019). A route navigation algorithm for pedestrian simulation based on grid potential field. *Advances in Mechanical Engineering*, 11(12), 1–13.
- Liu, X., & Lim, S. (2016). Integration of spatial analysis and an agent-based model into evacuation management for shelter assignment and routing. *Journal of Spatial Science*, 61(2), 283–298.
- Liu, Y., Okada, N., Shen, D., & Li, S. (2009). Agent-based flood evacuation simulation of life-threatening conditions using vitae system model. *Journal of Natural Disaster Science*, 31(2), 69–77.
- Lumbroso, D., & Davison, M. (2018). Use of an agent-based model and Monte Carlo analysis to estimate the effectiveness of emergency management interventions to reduce loss of life during extreme floods. *Journal of Flood Risk Management*, 11, S419–S433.
- Lumbroso, D., & di Mauro, M. (2008). Recent developments in loss of life and evacuation modelling for flood event management in the UK. *WIT Transactions on Ecology and the Environment*, 118, 263–272.
- Lumbroso, D., Gaume, E., Logtmeijer, C., Mens, M., & van der Vat, M. (2008). Evacuation and traffic management, integrated flood risk analysis and management methodologies. Floodsite Consortium Task 17 report number T17-07-02.
- Lumbroso, D., Sakamoto, D., Johnstone, W., Tagg, A., & Lence, B. L. (2011). The development of a life safety model to estimate the risk posed to people by dam failures and floods. Dams and Reservoirs, HRPP473.
- Lumbroso, D., & Vinet, F. (2012). Tools to improve the production of emergency plans for floods: Are they being used by the people that need them? *Journal of Contingencies and Crisis Management*, 20(3), 149–165.
- Lumbroso, D. M., Simm, J. D., Davison, M., White, K. D., & Durden, S. (2015). Use of agent-based modelling to validate hurricane evacuation planning. In *Coastal structures and solutions to coastal disasters joint conference (COPRI)*, pp. 321–329. 9–11 September 2015, Boston, MA.
- Mas, E., Koshimura, S., Imamura, F., Suppasri, A., Muhari, A., & Adriano, B. (2015). Recent advances in agent-based tsunami evacuation simulations: Case studies in Indonesia, Thailand, Japan and Peru. *Pure and Applied Geophysics*, 172(12), 3409–3424.

- McClymont, K., Morrison, D., Beevers, L., & Carmen, E. (2019). Flood resilience: A systematic review. *Journal of Environmental Planning and Management*, 63, 1–26.
- Mohler, B. J., Thompson, W. B., Creem-Regehr, S. H., Pick, H. L., & Warren, W. H. (2007). Visual flow influences gait transition speed and preferred walking speed. *Experimental Brain Research*, 181(2), 221–228.
- Néelz, S., & Pender, G. (2009). Desktop review of 2D hydraulic modelling packages, Science Report SC080035, Joint UK Defra/Environment Agency Flood and Coastal Erosion. Risk Management R&D Program.
- Padgham, L., Horne, R., Singh, D., & Moore, T. (2014). Planning for sandbagging as a response to flooding: A tool and case study. *Australian Journal of Emergency Management (AJEM)*, 29, 26–31.
- Richmond, P., Coakley, S., & Romano, D. M. (2009). A high performance agent based modelling framework on graphics card hardware with CUDA. In *Proceedings of the 8th International Conference on Autonomous Agents and Multiagent Systems*, pp. 1125–1126. 10–15 May 2009, Budapest, Hungary.
- Sen Nag, O. (2018). The largest shopping malls in the United Kingdom [online]. WorldAtlas. Retrieved from <https://www.worldatlas.com/articles/the-largest-shopping-malls-in-the-unit-ed-kingdom.html>.
- Shirvani, M., Kesserwani, G., & Richmond, P. (2020). Agent-based modelling of pedestrian responses during flood emergency: Mobility behavioural rules and implications for flood risk analysis. *Journal of Hydroinformatics*, 22(5), 1078–1092. doi.org/10.2166/hydro.2020.031
- Tonn, G. L., & Guikema, S. D. (2018). An agent-based model of evolving community flood risk. *Risk Analysis*, 38(6), 1258–1278.
- Toro, E. F. (2001). *Shock-capturing methods for free-surface shallow flows*. New York, NY: Wiley.
- Tugba, S. (2018). Leading twenty shopping centers in the United Kingdom (UK) as of June 2018, by size (in square meters) [online]. Statista. Retrieved from <https://www.statista.com/statistics/319446/top-shopping-centres-by-size-united-kingdom-uk>.
- United States Department of Agriculture. (2018). Module 207-hydrograph development. [online]. Natural Resources Conservation Service. Retrieved from https://www.nrcs.usda.gov/Internet/FSE_DOCUMENTS/stelprdb1083020.pdf.
- Wang, Y., Liang, Q., Kesserwani, G., & Hall, J. W. (2011). A 2D shallow flow model for practical dam-break simulations. *Journal of Hydraulic Research*, 49(3), 307–316.
- Wedawatta, G., & Ingirige, B. (2012). Resilience and adaptation of small and medium-sized enterprises to flood risk. *Disaster Prevention and Management: An International Journal*, 21(4), 474–488.
- Williamson, K. (2010). How sandbags work [online]. Howstuffworks. Retrieved from <https://science.howstuffworks.com/nature/natural-disasters/sandbag.htm>.
- Willis, T., Wright, N., & Sleigh, A. (2019). Systematic analysis of uncertainty in 2D flood inundation models. *Environmental Modelling & Software*, 122, 104520.
- Wirtz, P., & Ries, G. (1992). The pace of life-reanalysed: Why does walking speed of pedestrians correlate with city size? *Behaviour*, 123(1–2), 77–83.
- Zischg, A. (2018). Floodplains and complex adaptive systems—Perspectives on connecting the dots in flood risk assessment with coupled component models. *Systems*, 6(2), 9.

How to cite this article: Shirvani M, Kesserwani G, Richmond P. Agent-based simulator of dynamic flood-people interactions. *J Flood Risk Management*. 2021;14:e12695. <https://doi.org/10.1111/jfr3.12695>

APPENDIX

Validation of the non-sequential hydrodynamic model on FLAMEGPU

Two academic dam-break flow tests were used to verify the FLAMEGPU implementation of Equation (2) in updating the state of floodwater stored in the grid of flood agents. The first test considered symmetric 2D water propagation over a flat, frictionless, and initially wet area, and the second involved a wave propagation over a rough, initially dry area including three mounds. FLAMEGPU simulations were run on a grid of 128×128 flood agents. The results were compared to those of a sequential counterpart implementation on MATLAB and with reference predictions reported in the literature.

Radial dam-break flow

This test is often used to verify the implementation of newly developed shock-capturing flood models (Toro, 2001; Wang et al., 2011). The wave propagation happens after instantaneous removal of an imaginary cylinder-shaped dam located in the centre of a $40 \text{ m} \times 40 \text{ m}$ square area, causing a circular wave moving outwards from the centre. The thin 2.5 m radius circular wall of this dam retained an initial column of water 2.5 m deep. The rest of the area outside the dam is covered with 0.5 m of still water. A reference solution was

produced by solving the shallow water equation along the radial direction $r = \sqrt{x^2 + y^2}$ (Toro, 2001) by a second-order accurate scheme over a fine mesh made of $1,001 \times 1,001$ rectangular elements (Wang et al., 2011). Figure A1 compares the outputs produced by the non-sequential hydrodynamic model on FLAMEGPU to those produced by the sequential counterpart on MATLAB and the reference solution, in terms of water depth (h) and unit-width discharge ($q = hu$) cross sections along the radial direction at times $t = 1.4 \text{ s}$ and $t = 4.7 \text{ s}$ (following Toro, 2001 and Wang et al., 2011). The predicted water depth and discharge preserve the radial symmetry at both output times $t = 1.4 \text{ s}$ and $t = 4.7 \text{ s}$, and the outputs of the non-sequential hydrodynamic model were identical to those the sequential counterpart, both agreeing well with the reference solution. The discrepancies relative to the reference solution are expected as the latter was computed on a mesh resolution that is eight times finer and using a higher-order accurate solver.

Dam-break flow over terrain with wetting-and-drying

The non-sequential hydrodynamic model on FLAMEGPU was then applied to reproduce dam-break flows over a rough terrain with uneven ground elevation. This test was used to verify the robustness of its implementation for handling wetting-and-drying and step-terrain slopes. It

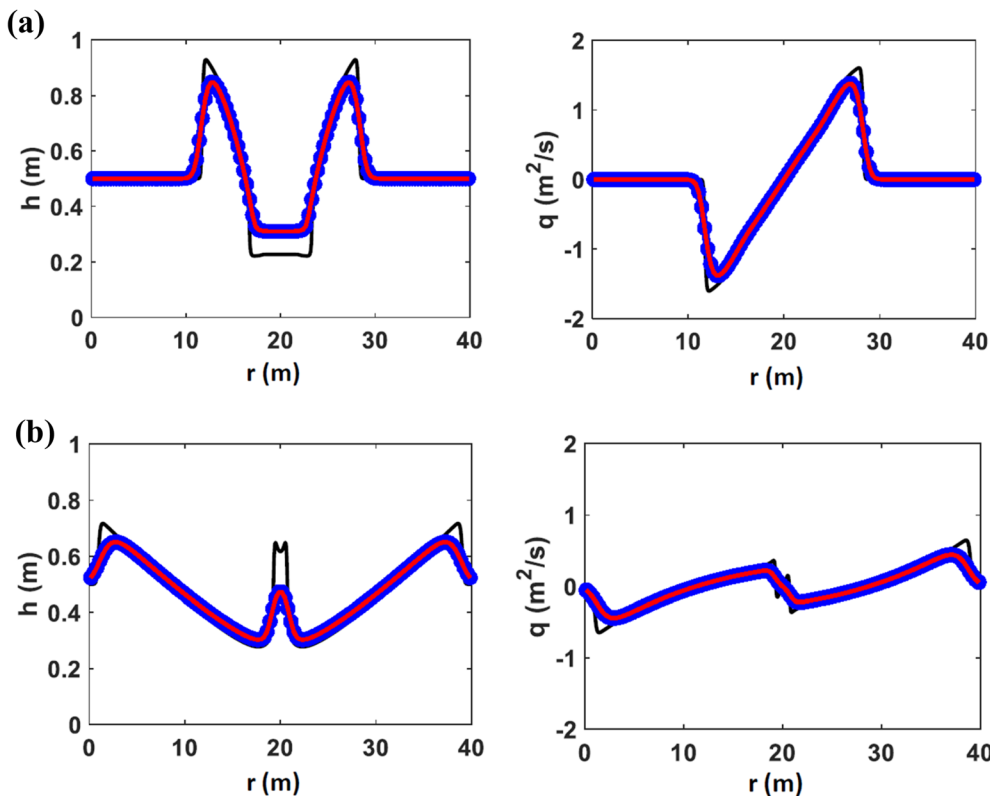
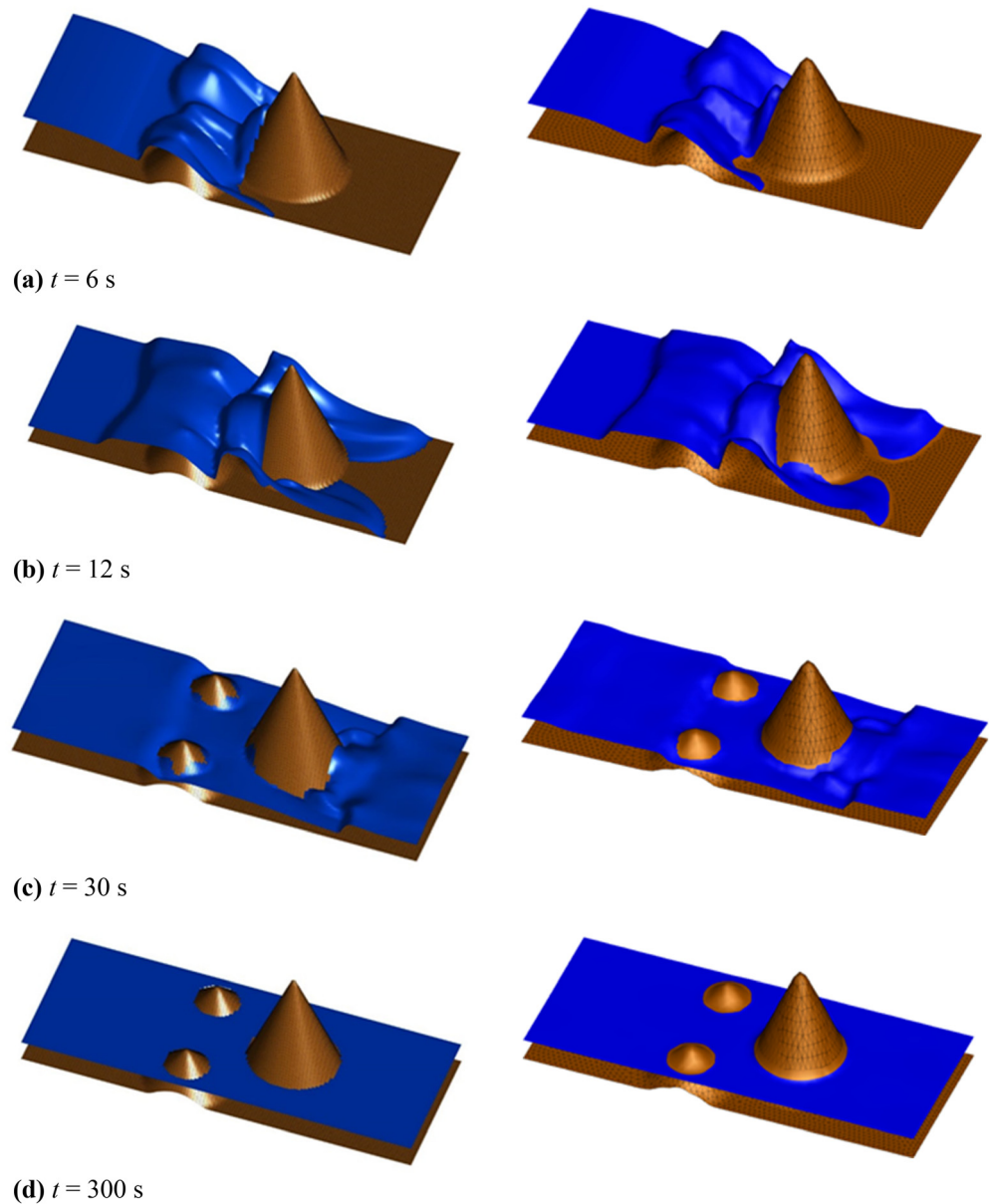


FIGURE A1 Profiles of water depth and unit-width discharge simulated by the non-sequential hydrodynamic model on FLAMEGPU (red line) against those simulated by the sequential model counterpart on MATLAB (blue circle-marked line) and the reference solution (solid black line)

FIGURE A2 Dam-break flow over terrain with wetting-and-drying. Free-surface elevation maps simulated by the non-sequential hydrodynamic model on FLAMEGPU (left) compared to the simulated results reported in Huang et al., 2013 (right)



assumes a dam-break wave propagating over a $75 \text{ m} \times 30 \text{ m}$ closed area with an initially dry floodplain including three mounds. The imaginary dam was located along $x = 16 \text{ m}$ locking an initial body of water with a height of 1.875 m . The roughness is represented by Manning coefficient $n_M = 0.018 \text{ s m}^{-1/3}$. Figure A2 (left) shows the simulated water surface elevation produced at the same output times as the results in Huang et al. (2013),

also shown in Figure A2 (right). As shown in Figure A2, the outputs delivered by the non-sequential hydrodynamic model on FLAMEGPU were similar to those of Huang et al. (2013), both demonstrating capability to capture wave reflections, wetting-and-drying fronts, and to conserve mass as the dam-break flood ultimately settles decelerated by friction effects.